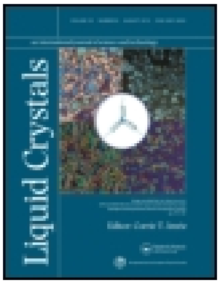

Liquid Crystals
Publication details, including instructions for authors and subscription information:
http://www.tandfonline.com/loi/tlct20

# A transflective liquid crystal display using polymer stabilised vertical alignment mode

Young Jin Lim [a], Se Hyun Lim [a], Nam Ho Cho [a], Ki-Chul Shin [b], Hee Seop Kim [b], Seung Hee Lee [a] & Gi-Dong Lee [c]

[a] Department of BIN Fusion Technology and Department of Polymer Nano-Science and Technology, Chonbuk National University, Jeonbuk, Korea

[b] LCD R&D Center, LCD Business of Samsung Electronics, Youngin, Gyeonggi-Do, Korea

[c] Department of Electronics Engineering, Dong-A University, Pusan, Korea

Version of record first published: 09 May 2012.

To cite this article: Young Jin Lim, Se Hyun Lim, Nam Ho Cho, Ki-Chul Shin, Hee Seop Kim, Seung Hee Lee & Gi-Dong Lee (2012): A transflective liquid crystal display using polymer stabilised vertical alignment mode, Liquid Crystals, 39:8, 911-915

To link to this article: http://dx.doi.org/10.1080/02678292.2012.686636

*Liquid Crystals,*
Vol. 39, No. 8, August 2012, 911–915



# A transflective liquid crystal display using polymer stabilised vertical alignment mode

Young Jin Lim[a], Se Hyun Lim[a], Nam Ho Cho[a], Ki-Chul Shin[b], Hee Seop Kim[b], Seung Hee Lee[a]* and Gi-Dong Lee[c]*

[a]*Department of BIN Fusion Technology and Department of Polymer Nano-Science and Technology, Chonbuk National University, Jeonbuk, Korea;* [b]*LCD R&D Center, LCD Business of Samsung Electronics, Youngin, Gyeonggi-Do, Korea;* [c]*Department of Electronics Engineering, Dong-A University, Pusan, Korea*

(*Received 12 March 2012; final version received 16 April 2012*)

A transflective liquid crystal display using polymer-stabilised vertical alignment mode with fishbone-shaped electrode structure is proposed. Using the polymer stabilisation technique and patterned direction of pixel electrode structure, initial surface tilt angle and azimuthal angle can be well defined such that the liquid crystal is almost vertically aligned in the transmissive part while it has a certain pretilt angle that satisfies effective retardation of $\lambda/4$ with azimuthal direction of 45° with respect to the analyser in the reflective part. With optimisation of cell structures and surface tilt angles in the transmissive and reflective parts, a high performance transflective display showing excellent readability in any environment light conditions and single-gamma characteristic without using any retardation film or in-cell retarder can be achieved.

**Keywords:** transflective; vertical alignment; fishbone-shaped electrode; polymer stabilisation



## 1. Introduction

Liquid crystal displays (LCDs) have become the most commonly used not only in portable devices such as smart phones, tablet personal computers (PCs) and notebook PCs, but also in monitors, public information displays (PIDS) and televisions. Transflective LCDs are highly important devices in the portable displays and PIDs because they can exhibit a high image quality in any light environmental conditions. The required performance of transflective LCDs is good sunlight readability with sufficient brightness, low power consumption, wide-viewing angle and touch sensitivity. A number of studies have been made using several modes such as twisted nematic (TN) [1, 2], electrically controlled birefringence (ECB) [3–5], vertical alignment (VA) [6–11], fringe-field switching (FFS) [12–18] and in-plane switching (IPS) [19, 20]. Among them, liquid crystal cells driven by VA mode have merits in that it shows excellent dark state at normal direction and does not require a mechanical rubbing process on alignment layers. Many cell structures in transflective LCDs with VA mode have been proposed but still have some serious disadvantages such as use of a circular polariser, a multi-cell gap and use of compensation films.

To solve these problems, we propose a new concept of the transflective LCD using VA mode which adopts a fishbone-shape electrode and polymer stabilisation process. In the device, to achieve the transflective LCD without compensation film or in-cell retarder, the LC director is almost vertically aligned in the transmissive (T) part while it is aligned with an azimuthal angle of 45° with respect to the analyser in the reflective (R) part having a high surface pretilt angle ($\theta_p$) sufficient to allow retardation of $\lambda/4$ in the R-part to achieve a single cell gap. The surface pretilt angle is formed through polymerisation of an UV curable reactive mesogen (RM) [21–24] at the surface when the voltage is applied.

## 2. Switching principle and cell condition

Figure 1 shows a top and cross-sectional view of the proposed single gap transflective LCD using VA mode with a fishbone-shaped electrode structure. This structure uses a plane common electrode on a top substrate and a fishbone-shape pixel electrode on a bottom substrate. The directions of the pixel electrode are patterned to 45°, 135°, 225° and 315°, respectively. With bias voltage between the pixel and common electrodes, oblique electric fields, which have vertical and horizontal components, are generated and the vertically aligned LC director tilts downward along patterned electrode directions, that is, the LC director tilts in four diagonal azimuthal directions in the T-part whereas it tilts in two azimuthal directions in the R-part. In addition, the reflective electrode that is formed during gate electrode patterning exists below the pixel electrode with an embossing pattern above the electrode that plays diffuse reflection in the R-part [16, 25].

*Corresponding authors. Email: lsh1@chonbuk.ac.kr(SHL), gdlee@dau.ac.kr(GDL)

ISSN 0267-8292 print/ISSN 1366-5855 online

http://dx.doi.org/10.1080/02678292.2012.686636
http://www.tandfonline.com

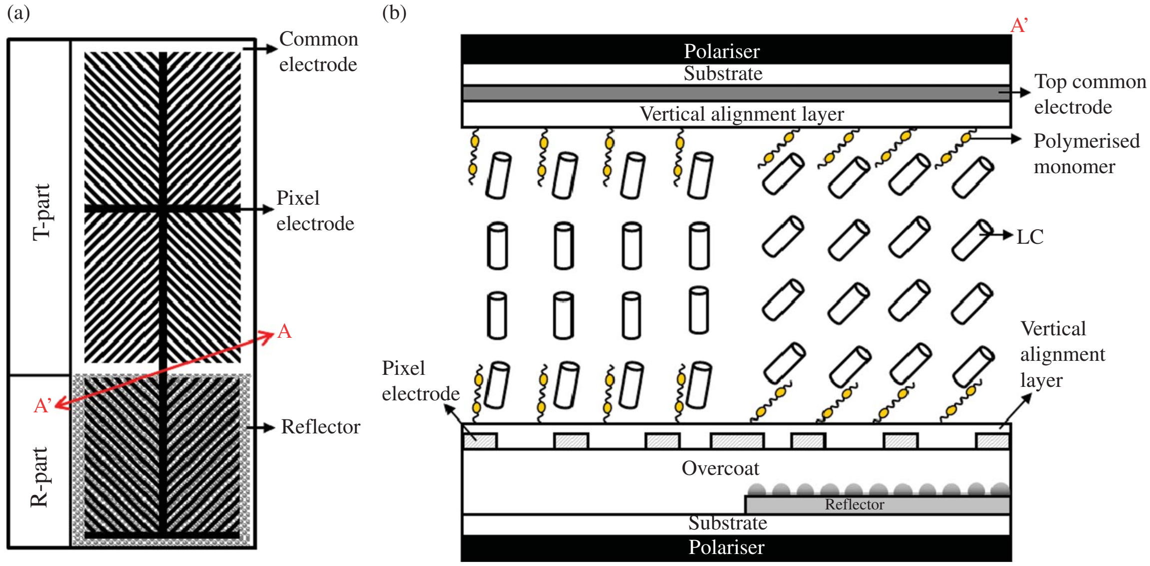


Figure 1. Schematic cell structure of the proposed transflective LCD driven by vertical electric field: (a) top and (b) cross-sectional view.

In the T-part, the transmittance ($T_T$) of the cell with a birefringent medium under two crossed polarisers is given by:

$$T_T = T_o \sin^2(2\psi)\sin^2(\pi d\Delta n_{eff}/\lambda) \qquad (1)$$

where $\psi$ is an angle between the polariser and LC director, $d$ is a cell gap and $\Delta n_{eff}$ is the effective birefringence of the LC layer and $\lambda$ is wavelength of an incident light. In the R-part, the reflectance ($R_R$) of the cell with a birefringent medium under a linear polariser is given by:

$$R_R = R_o \cos^2(2\pi d\Delta n_{eff}/\lambda) \qquad (2)$$

Therefore, the reflectance of the cell can be controlled by having an effective retardation layer of the LC layer, $d\Delta n_{eff}$. If it is equal to $\lambda/4$, the cell appears to be dark, and if it is equal to $\lambda/2$, it gives rise to a white state. However, because $\Delta n_{eff}$ is strongly wavelength-dependent, $\Delta n_{eff}$ should be optimised for each wavelength to achieve a good dark state. Here, the initial retardation of LC layer in the R-part can be adjusted by controlling the surface $\theta_p$ of the liquid crystal. It was known that a high surface $\theta_p$ of the liquid crystal on the vertical alignment layer can be achieved by polymerisation of the ultraviolet (UV) curable RM under a certain bias voltage as shown in Figure 1(b) and thus the effective cell retardation in the R-part can become $\lambda/4$ [18, 26].

The optical configuration of the proposed single cell gap transflective LCD using the VA mode with fishbone-shaped electrode structure is shown in

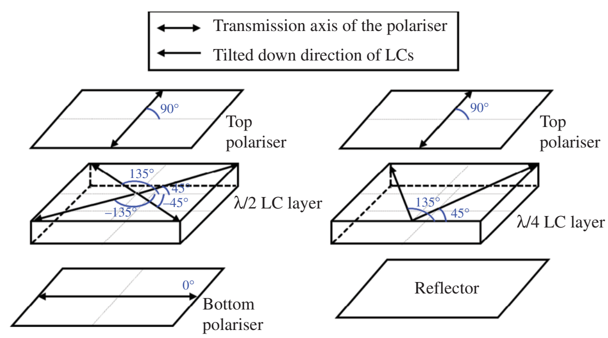


Figure 2. Optical cell configurations of the proposed transflective LCD: (a) T-part and (b) R-part.

Figure 2. In the T-part, the transmittance axes of polariser and analyser are 0° and 90°, respectively, and the LC directors are vertically aligned. In the absence of voltage, the linearly polarised light through the polariser passes through the LC layer without change of polarisation state. Thus it is blocked by the analyser, which results in a dark state. With a bias voltage, the LC directors are tilted down with four different azimuthal directions of 45°, 135°, 225° and 315° in each domain.

As a result, a white state is achieved with a condition of $d\Delta n_{eff} = \lambda/2$. In the R-part, the optic axes of the LC layer with $\lambda/4$ retardation make 45° and 135° with respect to the analyser, respectively, and the reflective electrode plays a role of a reflector. In the absence of voltage, the linearly polarised light through the analyser becomes circularly polarised after passing along the LC layer with $\lambda/4$ phase. After reflection, the circularly polarised light passes along the LC layer again and becomes linearly polarised with a 90° rotation. Then, the R-part appears to be dark. With a bias voltage, $d\Delta n_{eff}$ can be increased from $\lambda/4$ to $\lambda/2$ because the LC with negative dielectric anisotropy is used in the VA mode. In such a case, a linearly polarised light through the analyser becomes linearly polarised with a 90° rotation after passing along the LC layer and, after reflection, this light passes along the LC layer again, becoming linearly polarised with its axis coinciding with transmittance axis of analyser, giving rise to a white state.

## 3. Results and discussion

For electro-optic calculations, a commercially available LCD simulator (Shintech, Japan) was used. In both T- and R-parts, the width of each electrode in a fishbone-shaped pixel electrode is 4 µm and the distance between its electrodes is 4 µm. The cell gap of both the T- and R-parts in the first proposed cell structure is 4 µm, as shown in Figure 1(b). Here, a nematic LC with physical parameters such as dielectric anisotropy $\Delta\varepsilon = -4$, elastic constants $K_1 = 13.5$ pN, $K_2 = 6.5$ pN, $K_3 = 15.1$ pN, and birefringence $\Delta n = 0.09$ has been used, and the surface $\theta_p$ of the LC is 89° and 51° in the T- and R-parts, respectively. Here, for calculating the $R_R$ and $T_T$, a 2 × 2 extended Jones matrix was used [27]. The $T_T$s for single and parallel polarisers are assumed to be 41% and 35%, respectively.

The dark state characteristics of the device were analysed by calculating iso-luminance curves in light leakage according to surface $\theta_p$ and voltage-dependent $R_R$ and $T_T$ curves in all wavelengths as shown in Figure 3. The minimum light leakage in the R-part is found to be 2.4% when $\theta_p = 51°$ on both top and bottom substrates in all visible wavelengths as shown in Figure 3(a). Figure 3(b) shows that the operating voltages are 5 V and 2.4 V in the T- and R-parts, respectively. Here, there are two issues. The first is that voltage-dependent $T_T$ and $R_R$ curves do not match. The second is that there is relatively large light leakage in the R-part due to wavelength dispersion.

Figure 4 shows the optimised structure in the transflective LCD in order to solve those problems.

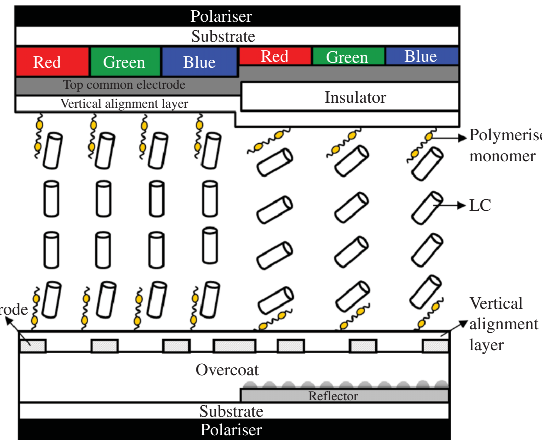


Figure 4. Schematic cell structures of single cell-gap transflective LCD with different surface pretilt angles in red, green and blue regions in the R-part.

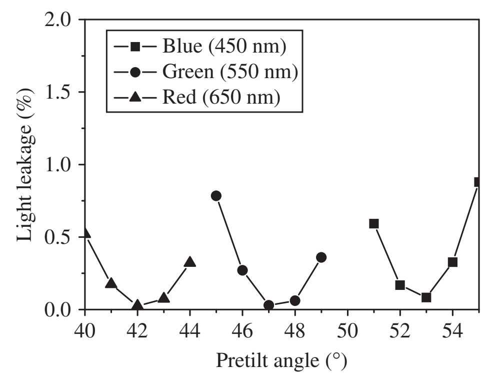


Figure 5. Light leakage according to surface pretilt angles at three different incident wavelengths in red, green and blue regions in the R-part.

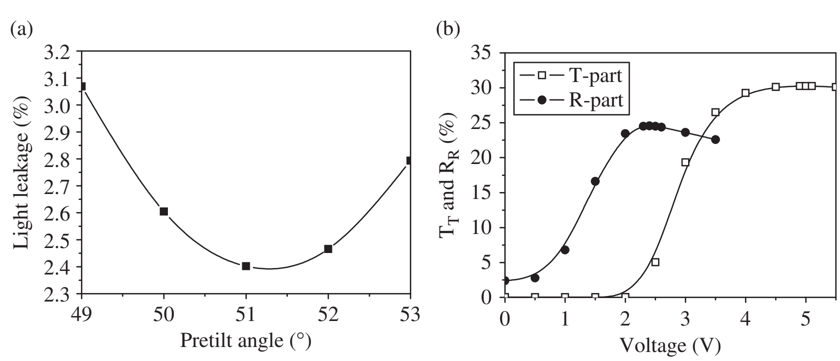


Figure 3. (a) Light leakage according to surface pretilt angles in the R-part and (b) voltage-dependent $R_R$ and $T_T$ curves at all visible wavelengths.

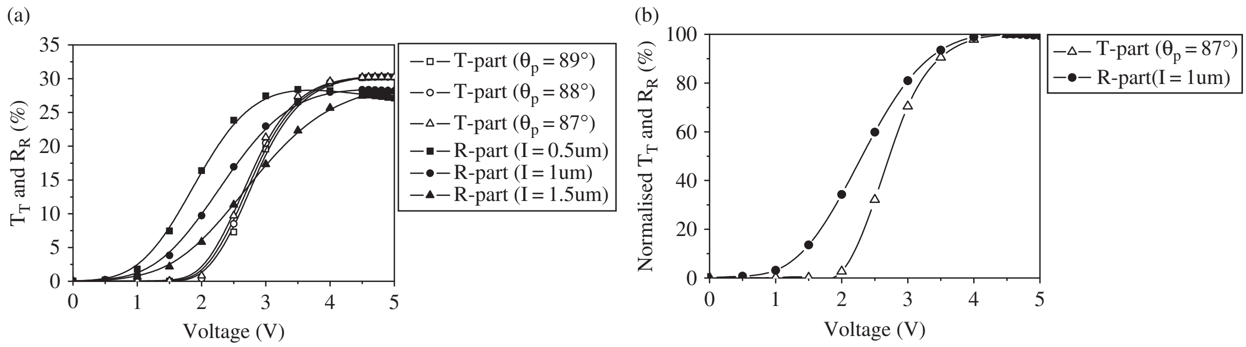


Figure 6. (a) Voltage-dependent $R_R$ and $T_T$ curves according to the pretilt angle and thickness of insulator layer in the T- and R-parts, respectively (b) normalized voltage-dependent $R_R$ and $T_T$ curves in the optimum gamma curve.

To obtain a single gamma curve, the thicknesses of the cell and colour filter in the T- and R-parts are set unlike and the insulator (I) was coated between the common electrode and vertical alignment layer in the R-part to make the cell gap different. In addition, conventional transflective LCDs have the same thickness of colour filter in the T- and R-parts which causes a different colour gamut in them because the light passes through the R-part twice. However, the optimised cell structure with a dual thickness of colour filter in the T- and R-parts will exhibit the same colour gamut in both.

In addition, we have further optimised the effective phase retardation value of the LC layer to minimise wavelength dispersion in the R-part. In order to match $d\Delta n_{\text{eff}} = \lambda/4$ at all wavelengths, surface pretilt angles in each red (650 nm), green (550 nm) and blue (450 nm) pixels are adjusted to be 42°, 47° and 53° when cell gap is 3.5 μm in the R-part. Such different pretilt angles can be easily achieved by applying different applied voltages in each pixel before UV exposure [18]. As shown in Figure 5, the light leakage is minimised with optimised pretilt angles in each pixel. From this result, we confirmed that the drop ratio of light leakage is 93% compared to the R-part with non-optimised pretilt angle.

Figure 6 shows calculated voltage-dependent $R_R$ and $T_T$ curves as a function of thickness of $I$ in the R-part and $\theta_p$ in the T-part and normalised voltage-dependent $R_R$ and $T_T$ curves to obtain an optimum single gamma curve in the T- and R-parts. As clearly indicated in Figure 6(a), when $I = 1$ μm in the R-part and $\theta_p = 87°$ in the T-part, the normalised voltage-dependent $R_R$ curve in the R-part is better matched to the normalised voltage-dependent $T_T$ curve in the T-part than other cases as shown in Figure 6(b). Though we can have better matching curves between voltage-dependent $T_T$ and $R_R$ curves with a lower value of $\theta_p$ in the T-part, such an approach causes a slight increase in light leakage in the dark state of the T-part. The increasing ratio of light leakage when $\theta_p = 87°$ is about 1.7% compared to light leakage when $\theta_p = 89°$ in the T-part. Therefore, the cell parameters could be chosen depending on the device's requirement if the high $R_R$ or single gamma curve is favoured or a high contrast ratio in the T-part is favoured.

## 4. Conclusions

A transflective vertical alignment liquid crystal display utilising a fishbone-shaped electrode and surface polymer stabilisation technology has been proposed. To achieve a good dark state and a single gamma curve, the surface pretilt angle on the each colour area of red, green, and blue in the reflective part was optimised and the insulator layer and pretilt angle in the reflective and transmissive parts are controlled, respectively. This new mode is expected to show a wide-viewing angle characteristic and good image quality without any compensation film or in-cell retarder.

## Acknowledgements

This study was supported by the World Class University programme (R31-20029) funded by the Ministry of Education, Science and Technology and research funds of Chonbuk National University in 2012.

## References

[1] Huang, Y.-P.; Su, M -J.; Shieh, H.-P.D.; Wu, S.-T. *SID Int. Symp. Dig. Tech. Pap.* **2003**, *34*, 86–89.
[2] Mak, H.-Y.; Xu, P.; Li, X.; Chigrinov, V.G.; Kwok, H.-S. *Jpn. J. Appl. Phys.* **2007**, *46*, 7798–7800.
[3] Baek, H.-I.; Kim, Y.-B.; Ha, K.-S.; Kim, D.-G.; Kwon, S.-B. *Proceedings of the 7th International Display Workshops*; Society for Information Display: Campbell, CA, 2001; 2000; pp. 41–44.
[4] Lim, Y.J.; Song, J.H.; Lee, S.H. *Jpn. J. Appl. Phys.* **2005**, *44*, 3080–3081.
[5] Hsiao, C.-C.; Lin, Y.-L.; Cheng, C.-S.; Hu, C.-J.; Huang, W.-M.; *SID Int. Symp. Dig. Tech. Pap.* **2008**, *39*, 1203–1206.

[6] Jisaki, M.; Yamaguchi, H. *Proceedings of the 8th International Display Workshops*; Society for Information Display: Campbell, CA, 2001; pp. 133–136.
[7] Kim, J.; Lim, Y.-W.; Lee, S.-D. *Jpn. J. Appl. Phys.* **2006**, *45*, 810–812.
[8] Lee, Y.-J.; Kang, S.-G.; Lee, T.-H.; Choi, Y.; Kim, H.-R.; Kim, J.-H. *Mol. Cryst. Liq. Cryst.* **2007**, *476*, 213–225.
[9] Lu, R.; Ge, Z.; Wu, S.-T. *Appl. Phys. Lett.* **2008**, *92*, 191102-1-3.
[10] Moon, J.-W.; Kang, W.-S.; Han, H.Y.; Kim, S.M.; Lee, S.H.; Jang, Y.G.; Lee, C.H.; Lee, G.-D. *Appl. Opt.* **2010**, *49*, 3875–3882.
[11] Kim, K.-B.; Gwag, J.S.; Lee, Y.-J.; Lee, H.J.; Kim, J.-H. *SID Int. Symp. Dig. Tech. Pap.* **2008**, *39*, 1920–1923.
[12] Jung, T.B.; Kim, J.C.; Lee, S.H. *Jpn. J. Appl. Phys.* **2003**, *42*, L464–L467.
[13] Jung, T.B.; Song, J.H.; Seo, D.-S.; Lee, S.H. *Jpn. J. Appl. Phys.* **2004**, *43*, L1211–L1213.
[14] Lim, Y.J.; Jeong, Y.H.; Choi, M O.; Jang, W.G.; Lee, S.H. *Jpn. J. Appl. Phys.* 2005, *44*, L1532–L1534.
[15] Song, J.H.; Lim, Y.J.; Lee, M.-H.; Lee, S.H.; Shin, S.-T. *Appl. Phys. Lett.* **2005**, *87*, 011108-1-3.
[16] Kim, H.Y.; Ge, Z.; Wu, S.-T.; Lee, S.H. *Appl. Phys. Lett.* **2007**, *91*, 231108-1-3.
[17] Lim, Y.J.; Lee, M.-H.; Lee, G.-D.; Jang, W.-G.; Lee, S.H. *J. Phys. D: Appl. Phys.* **2007**, *40*, 2759–2764.
[18] Her, J.H.; Shin, S.J.; Lim, Y J.; Park, K.H.; Lee, J.H.; Kim, B.K.; Lee, G.-D.; Lee, S.H. *Opt. Express* **2010**, *18*, 22842–22849.
[19] Song, J.H.; Lee, S.H. *Jpn. J. Appl. Phys.* **2004**, *43*, L1130–L1132.
[20] Lee, G.S.; Kim, J.C.; Yoon, T.-H. *Jpn. J. Appl. Phys.* **2007**, *46*, 289–292.
[21] Hanaoka, K.; Nakanishi, Y.; Inoue, Y.; Tanuma, S.; Koike, Y.; Okamoto, K. *SID Int. Symp. Dig. Tech. Pap.* **2004**, *35*, 1200–1203.
[22] Kim, S.G.; Kim, S.M.; Kim, Y.S.; Lee, H.K.; Lee, S.H.; Lee, G.-D.; Lyu, J.-J.; Kim, K. H. *Appl. Phys. Lett.* **2007**, *90*, 261910-1-3.
[23] Kim, S.M.; Cho, I.Y.; Kim, W.I.; Jeong, K.-U.; Lee, S.H.; Lee, G.-D.; Son, J.; Lyu, J.-J.; Kim, K.H. *Jpn. J. Appl. Phys.* **2009**, *48*, 032405-1-8.
[24] Kim, S.G.; Kim, S.M.; Kim, Y.S.; Lee, H.K.; Lee, S.H.; Lyu, J.-J.; Kim, K.H.; Lu, R.; Wu, S.-T. *J. Phys. D: Appl. Phys.* **2008**, *41*, 055401-1-4.
[25] Kang. S.-G.; Kim, S.-H.; Song, S.-C.; Park, W.-S.; Yi, C.; Kim, C.-W.; Chung, K.-H. *SID Int. Symp. Dig. Tech. Pap.* **2004**, *35*, 31–33.
[26] Lim, Y.J.; Chin, M.K.; Kim, J.H.; Her, J.H.; Jin, H.S.; Kim, B.K.; Lee, S.H. *J. Phys. D: Appl. Phys.* **2009**, *42*, 145412-1-5.
[27] Lien, A. *Appl. Phys. Lett.* **1990**, *57*, 2767–2769.